Available online at www.sciencedirect.com
ScienceDirect
Nuclear Medicine and Biology 35 (2008) 159–169
NUCLEAR MEDICINE — AND — BIOLOGY
www.elsevier.com/locate/nucmedbio

Isostructural fluorescent and radioactive probes for monitoring neural stem and progenitor cell transplants

Paul Schaffer[a], Jacqueline A. Gleave[b], Jennifer A. Lemon[c], Leslie C. Reid[d], Laura K.K. Pacey[b], Troy H. Farncombe[e], Douglas R. Boreham[c], Jon Zubieta[f], John W. Babich[g], Laurie C. Doering[b], John F. Valliant[c,d,*]

[a]*McMaster Nuclear Reactor, McMaster University, Hamilton, Ontario, Canada L8S 4K1*
[b]*Department of Pathology and Molecular Medicine, McMaster University, Hamilton, Ontario, Canada L8N 3Z5*
[c]*Department of Medical Physics and Applied Radiation Sciences, McMaster University, Hamilton, Ontario, Canada L8S 4K1*
[d]*Department of Chemistry, McMaster University, Hamilton, Ontario, Canada L8S 4M1*
[e]*Department of Nuclear Medicine, Hamilton Health Sciences, Hamilton, Ontario, Canada L8N 3Z5*
[f]*Department of Chemistry, Syracuse University, Syracuse, NY 13244-4100, USA*
[g]*Molecular Insight Pharmaceuticals Inc., Cambridge, MA 02142, USA*

Received 25 July 2007; received in revised form 25 September 2007; accepted 2 November 2007

Abstract

A construct for tagging neurospheres and monitoring cell transplantations was developed using a new technology for producing luminescent and radiolabeled probes that have identical structures. The HIV1-Tat basic domain derivatives NAcGRKKRRQRRR(SAACQ)G (SAACQ-**1**) and [NAcGRKKRRQRRR(Re(CO)$_3$SAACQ)G]$^+$ (ReSAACQ-**1**) were prepared in excellent yields using the single amino acid chelate-quinoline (SAACQ) ligand and its Re(I) complex and conventional automated peptide synthesis methods. The distribution of the luminescent Re probe, using epifluorescence microscopy, showed that it localized primarily in the cell nucleus with a significant degree of association on the nuclear envelope. A smaller amount was found to be dispersed in the cytoplasm. The ^{99m}Tc analogue was then prepared in 43±7% (n=12) yield and very high effective specific activity. Following incubation, average uptake of the probe in neurospheres ranged between 10 and 20 Bq/cell. As determined by colorimetric assays, viability for cells labeled with high effective specific activity ^{99m}TcSAACQ-**1** was 97±4% at 2 h postlabeling and 85±25% at 24 h postlabeling for incubation activities ranging from 245 to 8900 Bq/cell. DNA analysis showed that at these levels, there was no significant difference between the extent of DNA damage in the treated cells versus control cells. A series of preliminary SPECT/CT studies of transplants in mice were performed, which showed that the strategy is convenient and feasible and that it is possible to routinely assess procedures noninvasively and determine the number of cells transplanted.

Keywords: Neurospheres; Imaging; Technetium; Transplants; Peptide

1. Introduction

Neural stem cells (NSCs) have the ability to differentiate into neurons, astrocytes and oligodendrocytes in vivo [1] and are therefore under intense investigation as treatments for neurodegenerative diseases [2,3]. Unfortunately, the success of NSC transplantations in animal models and patients has been highly variable, which is due in large part to difficulties in achieving accurate, reproducible and efficient graft placements. Despite the development of several methods for long-term tracking of stem cell migration, better in vivo imaging strategies for routine monitoring and recording of implant procedures are needed in order to establish greater experimental controls in both preclinical and clinical studies. Here, we report the development of a dual-modality imaging strategy to study labeled neurospheres and monitor cell transplantations, which is based on a new technology for producing

* Corresponding author. Department of Chemistry, McMaster University, 1280 Main St. West, Hamilton, Ontario, Canada L8S 4M1. Tel.: +1 905 525 9140x22840; fax: +1 905 522 7776.
E-mail address: valliant@mcmaster.ca (J.F. Valliant).

0969-8051/$ – see front matter © 2008 Elsevier Inc. All rights reserved.
doi:10.1016/j.nucmedbio.2007.11.001

luminescent and radiolabeled probes that have identical structures. Using this approach, we developed a labeled peptide that can efficiently and noninvasively tag neurospheres so that transplants can be assessed both qualitatively and quantitatively using small-animal imaging techniques.

Recent studies suggest that cell transplantations are performed correctly only 50% of the time despite the use of surgical aids such as ultrasound-guided injection [4]. In the case of neurological applications, better methods are needed to assess stem cell transplants in order to eliminate subject-to-subject and technique-oriented variability and to provide a permanent record of the initial location and spatial distribution of transplanted cells. This information, when correlated with therapeutic outcomes, can be used to identify the most effective and reproducible implantation techniques. Dual-modality imaging methods such as SPECT/CT, which combine both anatomical and molecular imaging techniques, offer a convenient and accurate means of monitoring stem cell therapies. Once an appropriate cell-labeling system is developed (vide infra), scintigraphic imaging coupled with X-ray CT can provide both qualitative and quantitative information about cell transplants. It is noteworthy that for preclinical studies, imaging experiments can be performed using high-resolution small-animal SPECT/CT scanners, where the developed techniques can subsequently be adapted for monitoring studies in patients [5].

A variety of strategies for labeling stem cells with radioisotopes have been developed to monitor cell migration by nuclear imaging methods [5–14]. Unfortunately, these methods suffer from limitations that prevent their routine use in preclinical research and in clinical trials. These include the use of agents that are expensive or not readily available and those that have poorly characterized biological properties in terms of the impact on cell viability or low cell uptake. Poor uptake results in the need to use a large number of cells to achieve sufficient sensitivity during imaging studies. This is particularly problematic for small-animal neurological experiments where only a limited number of cells can be used so as to avoid host tissue damage. It is clear that new and more readily accessible approaches for labeling stem cells that have well-characterized biological effects and improved tracer uptake are needed to routinely monitor implant procedures. The development and validation of such a system, based on a uniquely labeled permeation peptide, are described here along with its application in assessing neurosphere transplants in mice using small-animal SPECT/CT.

2. Materials and methods

2.1. Maintenance of animal colonies

All animal experiments were carried out in accordance with the guidelines set out by the Canadian Council on Animal Care and were approved by the Animal Research Ethics Board of McMaster University.

2.2. Chemicals and instrumentation

Unless otherwise stated, all reagents and solvents were of ACS grade or higher and used without further purification. Polystyrene-based *N*-α-9-fluorenylmethoxycarbonyl (Fmoc)-glycine loaded Wang resin (0.82 mmol g^{-1}, 1% divinylbenzene, 200–400 mesh) was obtained from Nova-Biochem Inc. Fmoc-protected amino acids were purchased from NovaBiochem Inc., Bachem Inc. or Advanced ChemTech Inc. All peptides were prepared on an Advanced ChemTech 348-Ω Peptide Synthesizer using a 40-well reaction vessel. Peptides were analyzed by electrospray mass spectrometry, performed on a Quattro LC (Micromass, England) triple-quadrupole instrument. IR spectra were acquired as KBr pellets on a Perkin-Elmer Series 1600 FT-IR spectrometer. Glassware was silanized by pretreating with Sigmacote (Aldrich, Canada) followed by air and oven drying overnight.

2.3. HPLC

Analytical HPLC was performed using a Varian Pro Star model 330 PDA detector, a model 230 solvent delivery system and a Microsorb C-18 column (4.6×250 mm, 300 Å to 5 μm). The mobile phase consisted of either Method A or Method B. For Method A, Solvent A=H_2O containing 0.1% TFA and Solvent B=acetonitrile containing 0.05% TFA. The elution protocol consisted of the following: 0–20 min, 90% A to 20% A; 20–22.5 min, 20% A to 0% A; 22.5–25 min, 0% A; 25–30 min, 0% A to 90% A. For Method B, Solvent A=triethylammonium phosphate buffer (pH≅2–2.5) and Solvent B=CH_3OH. The elution protocol consisted of the following: 0–3 min, 100% A; 3–6 min, 100% A to 75% A; 6–9 min, 75% A to 67% A; 9–20 min, 67% A to 0% A; 20–22 min, 0% A; 22–25 min, 0% A to 100% A; 25–30 min, 100% A. The flow rate was 1.0 ml min^{-1}, and all runs were monitored at λ=254. Radio-HPLC experiments were performed on a Varian Pro Star model 230 HPLC instrument coupled to a Bio-Rad IN/US γ-detector using a Cobert Xpertek C-18 nucleosil column (4.6×200 mm, 300 Å to 5 μm).

Semipreparative HPLC was performed using a Varian Pro Star model 330 PDA detector, a model 230 solvent delivery system and a Phenomenex C-18 Partisil 10-ODS-3 column (9.8×500 mm, 300 Å to 5 μm). The solvents and elution profile were identical to those of Method A (above). The flow rate was 4.0 ml min^{-1}, and runs were monitored at λ=254.

2.4. Solid-phase peptide synthesis

Fmoc-glycine loaded Wang resin (100 mg, 0.82 mmol/g) was added to the reaction vessel, suspended in DMF (2 ml/well) and shaken at 600 rpm for 1 min. The wells were subsequently filtered, suspended in THF (2 ml/well), shaken at 600 rpm for 1 min and drained for 90 s. The THF wash was repeated two more times. The DMF wash was then repeated a final two times to complete the general wash cycle. This procedure was used between every deprotection and coupling step. Fmoc

deprotection was brought about through the addition of 20% v/v piperidine–DMF solution to the active vessels (2 ml/well) and shaking for 5 min at 600 rpm. Following filtration, the process was repeated, shaking for 10 min. The deprotected resin-bound amino acid was washed using the general wash procedure and subsequently coupled to the next Fmoc-protected amino acid using a standard HBTU coupling protocol. Coupling reactions initially involved adding DMF (200 μl) to the active vessels followed by the addition of a fourfold excess of the protected amino acid as a 0.5-M solution in DMF. Four equivalents of HBTU as a 0.5-M solution in DMF was then added, followed by a fourfold excess of DIPEA as a 2.0-M solution in DMF. The reaction block was subsequently shaken for 80 min at 600 rpm. Following filtration, the resin was washed using the general washing procedure prior to the start of the next cycle.

Peptides were cleaved from the resin support using a TFA mixture containing EDT (2%), water (2%) and TIS (2%). The cleavage solution was cooled to 0°C and added to the resin. The mixture was allowed to warm to room temperature and agitated for 24 h. The suspension was filtered into cold diethyl ether, and the resulting precipitate was centrifuged at 3000 rpm at 5°C for 30 min. The pellet was subsequently washed with cold diethyl ether (3×25 ml), dissolved in distilled deionized water and lyophilized, yielding a white solid for NAcGRKKRRQRRR(SAACQ)G (SAACQ-**1**) and an off-white solid for $[NAcGRKKRRQRRR(Re(CO)_3\text{-}SAACQ)G]^+$ (ReSAACQ-**1**).

SAACQ-**1** showed the following: FTIR (KBr, cm^{-1}): 3309, 3197, 2954, 1668, 1546, 1431, 1204 and 1135; ESMS (*m/z*, positive ion): 1906 $[M+H]^+$; HPLC: T_R=10.7 min (Method A). ReSAACQ-**1** showed the following: FTIR (KBr, cm^{-1}): 3312, 3198, 2955, 2035, 1933, 1665, 1546 and 1433; ESMS (*m/z*, positive ion): 2176 $[M+H]^+$; HPLC: T_R=13.8 min (Method A).

2.5. Preparation of $[^{99m}Tc(CO)_3(OH_2)_3]^+$

A 10-ml multidose vial containing $K_2[BH_3{\cdot}CO_2]$ (8.5 mg, 6.3×10^{-5} mol), $Na_2B_4O_7{\cdot}10H_2O$ (2.9 mg, 7.6×10^{-6} mol), Na/K-tartrate (15.0 mg, 5.3×10^{-5} mol) and Na_2CO_3 (4.0 mg, 3.8×10^{-5} mol) was fitted with a rubber septum and flushed with N_2 (g) for 15 min. ^{99m}Tc-generator eluate (370–1110 MBq, 10–30 mCi) in 900 μl of saline was added using a syringe, and the solution was heated to 95°C for 30 min. After cooling on an ice bath, the pH of the solution was adjusted to approximately 7.0–7.5 by the addition of HCl (65 μl of a 2.63-M solution of HCl). Quality control was performed by analytical HPLC (Method B): Yield: ≥95%.

2.6. Peptide labeling with ^{99m}Tc

An aliquot (100 μl) of AcGRKKRRQRRR(SAACQ)G (SAACQ-**1**) (1.0 mg, 5.3×10^{-7} mol) in 100 μl of distilled deionized water was added to the solution containing $[^{99m}Tc(CO)_3(OH_2)_3]^+$ using a syringe, and the reaction was heated at 72°C for 60 min. The mixture was subsequently cooled in an ice bath, and the product was isolated by using either a C_{18} Sep-Pak (Waters Inc.) for low specific activity or semipreparative HPLC (Method A) for high specific activity. Prior to use, the Sep-Pak was conditioned with absolute ethanol (10 ml), acetonitrile (10 ml), 1:1 acetonitrile/10 mM HCl (10 ml) and 10 mM HCl (10 ml). The reaction mixture was subsequently loaded, and the Sep-Pak slowly eluted into 1-ml fractions using 10 mM HCl (7×1 ml), 1:4 acetonitrile/10 mM HCl (2×1 ml), 1:1 acetonitrile/10 mM HCl (2×1 ml), 4:1 acetonitrile/10 mM HCl (2×1 ml) and acetonitrile (3×1 ml). The desired product eluted in fractions 9–13 (radiochemical yield=43±7%, radiochemical purity ≥98%).

2.7. Ligand challenge experiments

Ten microliters of a solution of cysteine (7.88 mg in 5 ml of ddH_2O) and histidine (7.76 mg in 5 ml of ddH_2O) was added to two separate vials, each containing 11.1 to 18.5 MBq (300 to 500 μCi) of purified ^{99m}TcSAACQ-**1** in 250 μl of 100 mM phosphate buffer. Both vials were incubated at 37°C and monitored by HPLC (Method A) over 24 h.

2.8. Preparation of neurospheres

CDI or B6.129.FMR1/FvBn mouse pups (1–3 days old) were decapitated, and the brain was removed and transferred to sterile artificial cerebrospinal fluid (aCSF) consisting of 0.012 M NaCl, 0.005 M KCl, 0.03 M $MgCl_2$, 0.026 M $NaHCO_3$, 0.01 M glucose and 0.097 mM $CaCl_2$ in dH_2O. The cerebellum was removed and the hemispheres were cut in the midsagittal plane. Each half was transferred to a tissue culture dish containing 3 ml of aCSF. The tissue was further cut into 0.5- to 1-mm^2 pieces and transferred to 1 ml of aCSF containing 0.13 mg kynurenic acid (Sigma), 0.66 mg hyaluronidase (Sigma) and 1.3 mg trypsin (Sigma). After incubation at 37°C in a shaking water bath for 1 h, the digested tissue was centrifuged at 730×*g* for 5 min and then transferred to a solution of trypsin inhibitor (Roche) 1 mg/ml in DMEM/F12 (Invitrogen) medium with glucose, HEPES buffer (Sigma), putrescene (Sigma), progesterone (Sigma), insulin–transferrin–sodium–selenite (Roche), B27 growth supplement, epidermal growth factor (Sigma), basic fibroblast growth factor (Sigma) and heparin (Sigma) and incubated for 10 min in a 37°C shaking water bath. The mixture was centrifuged at 730×*g* for 5 min. The resulting pellet was triturated and reconstituted in 12 ml of serum-free medium. The cell suspension was plated in two 24-well dishes (Falcon; 500 μl of cell suspension per well) and incubated in 95% O_2 and 5% CO_2 and passed every 5–7 days.

2.9. Labeling of neurospheres with ^{99m}TcSAACQ-*1*

Neurospheres were transferred from the 24-well dishes to 15-ml Falcon tubes and centrifuged at 730×*g* for 5 min. The resulting pellet was incubated in 2 ml of TrypLE Express (Invitrogen) and incubated at 37°C for 20 min in a shaking water bath. The mixture was centrifuged at 730×*g* for 5 min, and the pellet was transferred to 500 μl of

DMEM/F12 medium and triturated with a fire-polished, small borehole pipette. Cell counts were determined by mixing 16 μl of the cell suspension with 4 μl of trypan blue and counting phase bright cells with the aid of a hemacytometer. Cells were plated into 60×15 mm tissue culture dishes at a concentration of 10,000 cells/ml; 30× PBS was added to the solution containing ^{99m}TcSAACQ-**1** to give a 1× PBS solution of 0.01 M and subsequently added to the cells and incubated at 37°C in a 95% O_2/5% CO_2 incubator for 20 min. The labeled cells were transferred to a 15-ml siliconized glass centrifuge tube (VWR Canada) and centrifuged at 730×*g* for 5 min. The supernatant was removed, replaced with 2 ml of serum-free medium and centrifuged for 5 min at 730×*g*. The wash was removed and replaced with 2 ml of serum-free medium. Labeling efficiency was determined using a dose calibrator that had been calibrated using an NIST traceable standard over the range of activities employed. Control cells were prepared in an identical manner with 0.01 M PBS added instead of the labeled peptide.

2.10. Epifluorescence microscopy

Microscopy experiments were conducted with a Zeiss Axioskop 2 epifluorescence microscope. Visualization of ReSAACQ-**1** was achieved using a commercially available filter set consisting of a dichroic 360±40 nm excitation filter, a 400-nm dichroic long-pass filter and a 550-nm long-pass emission filter. Image analysis was performed with the Zeiss AxioVision 3.1 Imaging software package.

NSCs were isolated and prepared for labeling as described above. Specifically, approximately 20,000 cells/ml were incubated at 37°C for 120 min with 0.0712 or 0.0909 mg/ml of ReSAACQ-**1**. The cells were collected into 15-ml Falcon tubes and centrifuged for 5 min at 730×*g*. The supernatant

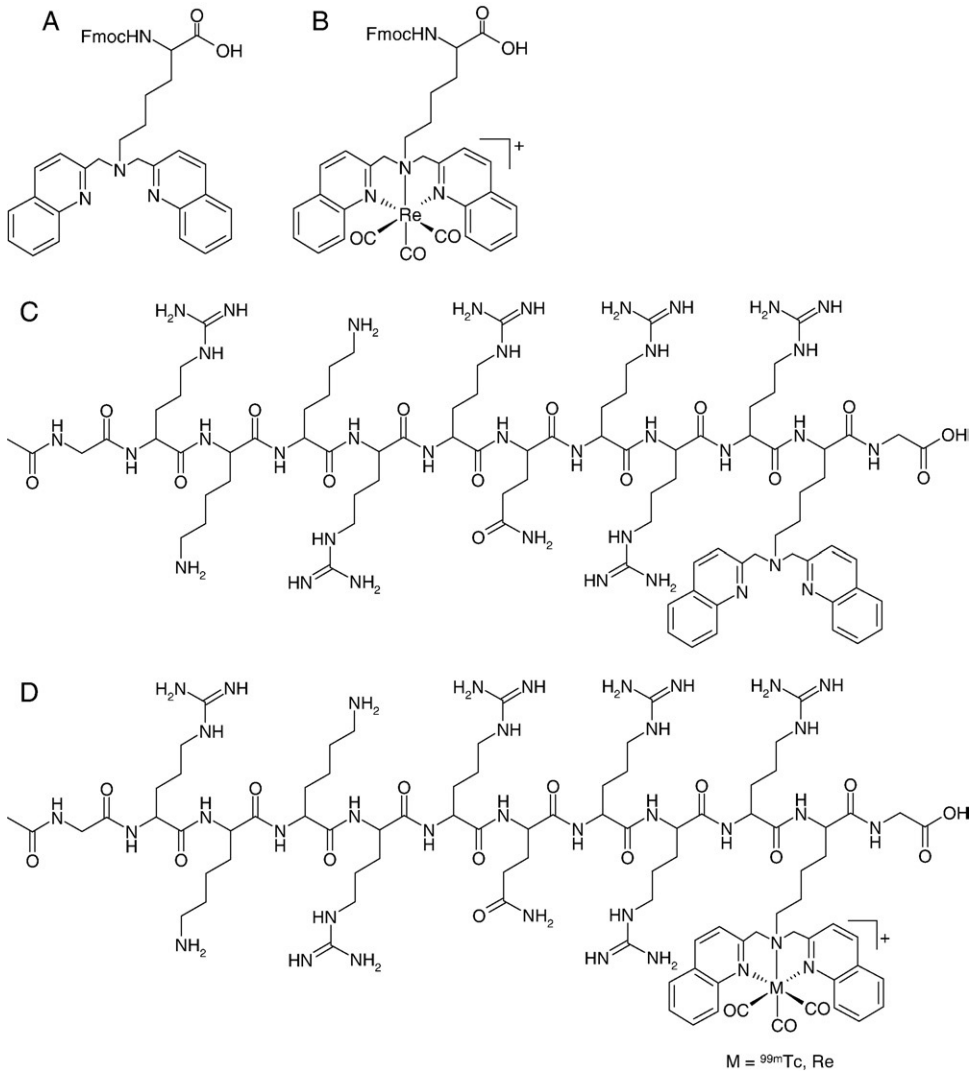

Fig. 1. (A) Fmoc-protected single amino acid (bis-quinoline) chelate (SAACQ) and (B) the corresponding Re complex $[Re(CO)_3SAACQ]^+$. Peptides (C) AcGRKKRRQRRR(SAACQ)G (SAACQ-**1**) and (D) $[AcGRKKRRQRRR(M(CO)_3SAACQ)G]^+$ (M=^{99m}Tc, ^{99m}TcSAACQ-**1**; M=Re, ReSAACQ-**1**).

was removed, and cells were fixed in 4% paraformaldehyde (PFA) for 5 min. The 4% PFA was diluted with 0.01 M PBS and centrifuged for 5 min at 730×*g*. The supernatant was removed, and the cells were washed with 0.01 M PBS. The cell pellet was suspended in 200 μl of dH_2O, and the cell suspension was placed on a glass slide and allowed to dry. The slides were mounted with DakoCytomation fluorescent mounting medium.

2.11. Single-cell gel electrophoresis

Comet assays were performed under alkaline conditions. Using a modified literature protocol [29,30], we diluted the cell culture 1:1 with 1% low melting point agarose (Fisher Scientific, Middletown, VA), prewarmed to 42°C. One hundred twenty microliters of this solution was cast into two individual wells of a two-well chamber (Nalge Nunc

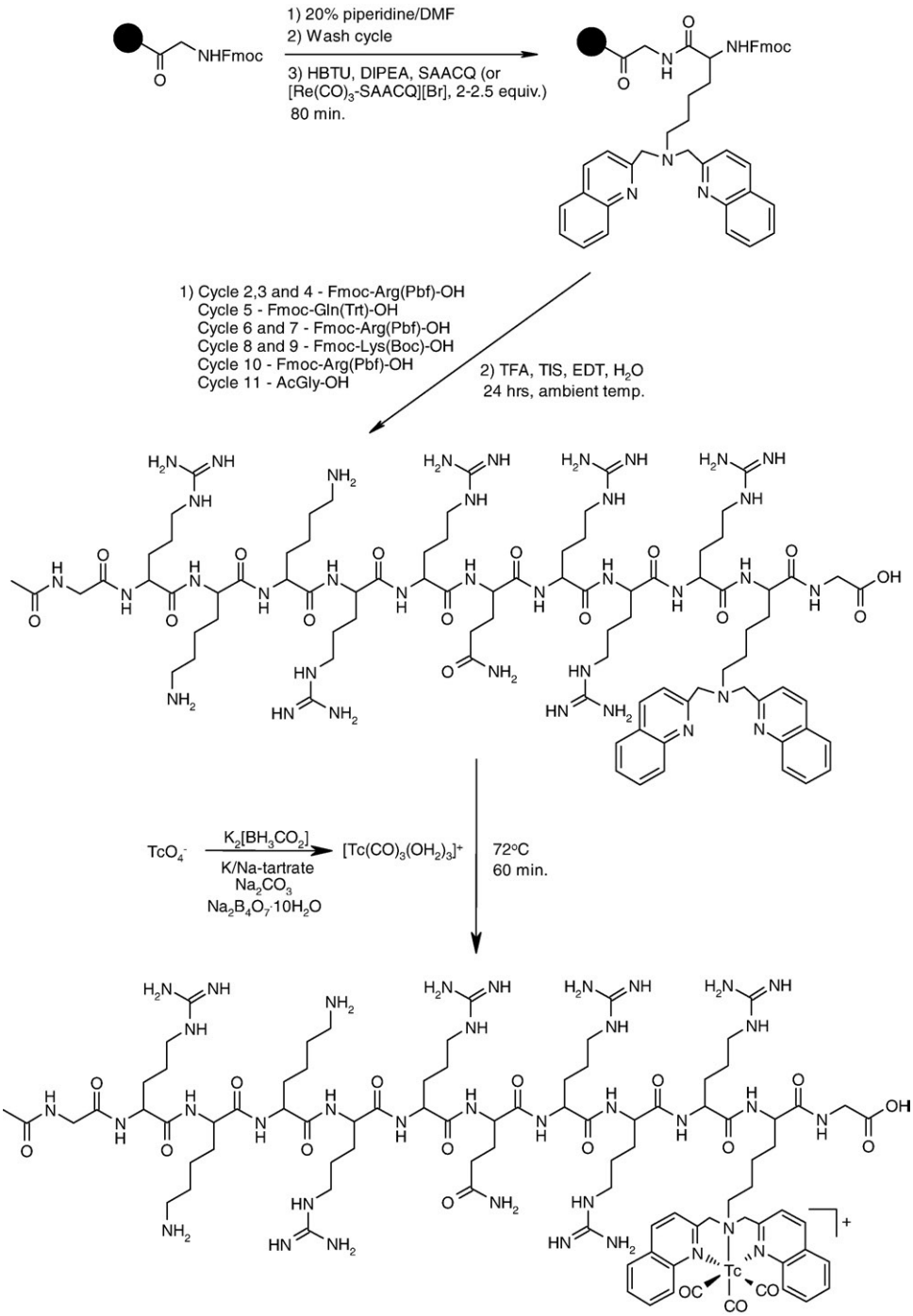

Fig. 2. Automated synthesis of SAACQ-**1** and subsequent labeling with $[^{99m}Tc(CO)_3(OH_2)_3]^+$ to generate ^{99m}TcSAACQ-**1**.

International, Rochester, NY) attached to GelBond film (Mandel Scientific, Guelph, ON). The gels were left to set at room temperature for 10 min; the two-well chamber form was then removed, and the gels were placed in lysis buffer [2.5 M NaCl, 100 mM tetrasodium ethylenediamine tetraacetate (EDTA), 10 mM Tris base, 1% *N*-lauroyl sarcosine, 1% Triton-X and 10% DMSO] and incubated at 37°C for 4 h. Gels were rinsed two times with 18.2 MΩ ultrapure water and placed in 4°C DNA unwinding buffer (10 M NaOH, 200 mM EDTA in 18 MΩ ultrapure water, pH>13), and the mixture was incubated at room temperature for 30 min. The gels were then placed in submarine agarose gel units (model HE-33, Hoefer, San Francisco, CA) containing 220 ml DNA unwinding buffer and electrophoresed for 10 min at 25 V. The gels were then rinsed two times in 1× TAE (40 mM Tris–acetate, 10 mM EDTA, 20 mM glacial acetic acid), dehydrated in absolute ethanol for a minimum of 2 h and air dried overnight. The gels were stained by immersion in 50 ml SYBR Gold nucleic acid stain (1:10,000 dilution in 18 MΩ ultrapure water) for 10 min. The gels were then rinsed in 18.2 MΩ water and mounted onto a microscope slide and covered with a glass coverslip. Cells were analyzed using a fluorescence microscope (Zeiss Axioplan 2, Carl Zeiss MicroImaging, Inc., Thornwood, NY) under ×200 magnification with an excitation wavelength of 520 nm and emission of 580 nm. Cells were classified as normal, damaged or apoptotic based on the DNA fragmentation pattern observed in the comet tail as previously described [15].

2.12. Animal imaging protocols

B6.129.FMR1/FvBn mice (approximately 20 g) were anesthetized by intraperitoneal injection of 150 mg/kg ketamine and 10 mg/kg xylazine. Labeled cells were loaded into a 10-µl Hamilton syringe and injected into the striatum in a volume of 3.0 µl of lactated Ringer's solution using a stereotaxic injection frame. The bilateral striatal injection was performed at +0.5 bregma, +1.5 ML, +2.5 DV and +0.5 bregma, −1.5 ML, +2.5 DV. The animals were then placed in the supine position on a standard bed of a GammaMedica X-SPECT preclinical imaging system. Image acquisition was performed using a dual-head detector system (125×125×125 mm reconstructed field of view). Whole-body SPECT imaging was performed using a low-energy, high-resolution collimator over a total of 64 angles around the body (32 angles per detector with 30 s per projection). Projection data were then reconstructed using a filtered back-projection algorithm into a three-dimensional representation of radiotracer distribution. As radiotracer quantitation was not deemed important at this stage, no corrections for radiotracer decay or photon attenuation were included.

Following whole-body imaging, high-resolution pinhole SPECT imaging was acquired over the head over several hours. This imaging utilized a pair of 1.0-mm pinhole collimators and acquired projections over 64 angles around the head (32 angles per detector). Initial studies involved sacrificing the animal and imaging the animal over several hours (16 h total). In this case, radiotracer decay was significant; hence, projection data were first decay corrected prior to reconstruction. For acquisitions of less than 2 h duration, projection data were not decay corrected prior to reconstruction. In all cases, the same iterative pinhole reconstruction algorithm was used for image reconstruction. As photon attenuation is considered relatively minor in a mouse head, no corrections for this effect were included.

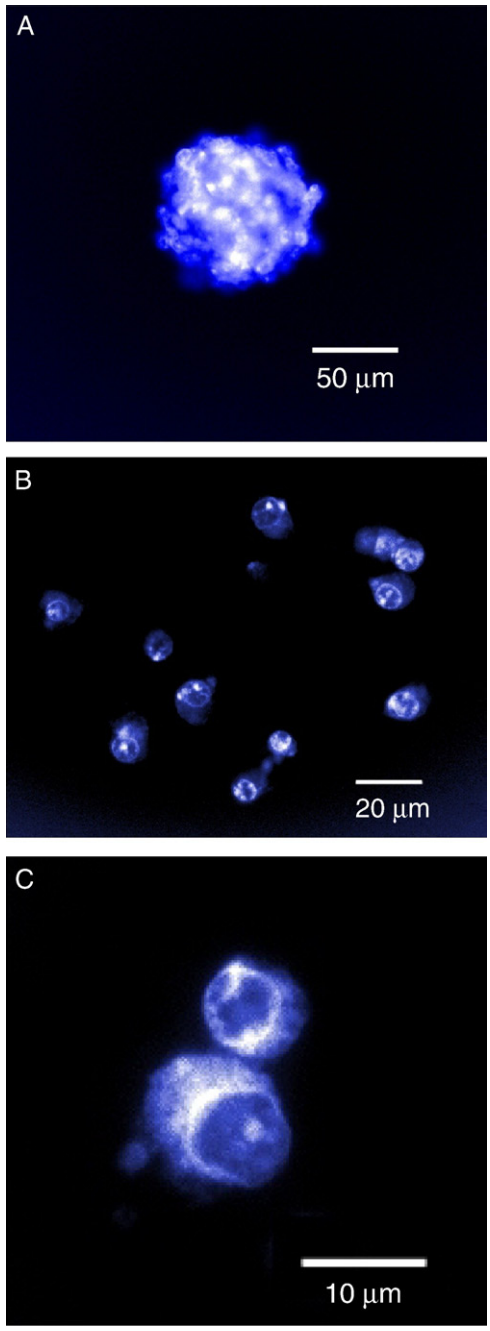

Fig. 3. Epifluorescent images of (A) a single neurosphere, (B) single-cell suspension at low magnification and (C) single-cell suspension at higher magnification. Cells were incubated with ReSAACQ-**1** for 2 h at 37°C.

For anatomical localization, an accurately coregistered volumetric X-ray CT image was obtained using the same scanner. A total of 256 projection measurements were acquired into a 1024×1024 array (100 μm pixel size), using 80-kVp X-rays and a tube current of 0.24 mA. To minimize animal dose, we used a 1.0-mm Al filter in order to remove low-energy X-rays. Projection data were reconstructed using a modified Feldkamp cone-beam reconstruction algorithm into a 512×512×512 array with a voxel size of 0.156 mm. Reconstructed SPECT and CT images were then coregistered and interpolated to 256×256×256 matrices covering the same field of view, so that image fusion could be performed. Image display and analysis were performed using Amide or Amira image visualization software.

3. Results and discussion

^{99m}Tc is the most widely used radionuclide in diagnostic medicine and is an attractive isotope for monitoring cell transplantation procedures. It has a reasonably long half-life (6 h) and is readily available in nearly all hospitals, making any ^{99m}Tc-derived stem-cell-tagging agent accessible to the general research community at a reasonable cost. This is an important consideration given the number of transplants done in a typical preclinical study. An additional advantage of using ^{99m}Tc is that it imparts a low dose burden, thereby limiting potential radiation damage to the labeled cells and the transplant subject. To facilitate labeling of stem cells, we prepared a derivative of a permeation peptide derived from the HIV1-Tat basic domain (GRKKRRQRRR$_{48–57}$) that can be efficiently radiolabeled with ^{99m}Tc. Permeation peptides were selected because they can concentrate a variety of molecular cargo, including nanoparticles [16–19], quantum dots [20] and radionuclides [18,21], into an assortment of cell types. In addition, they typically localize material intracellularly as opposed to concentrating in the lipid bilayer (the common target of the majority of existing cell-labeling strategies), which helps prevent premature loss of the label in vivo. The actual sequence selected, which is an N-acetylated analogue, has been shown to be a highly efficient delivery vector that has the necessary stability in vitro and in vivo [22].

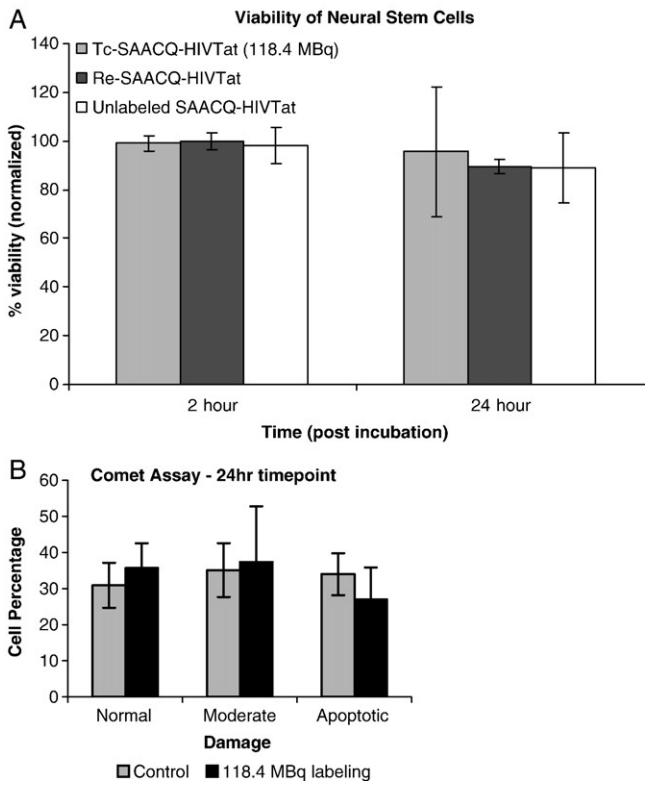

Fig. 4. Viability of neurosphere cells labeled with ^{99m}TcSAACQ-**1**. (A) Results of dye-exclusion assay for cells incubated with ^{99m}TcSAACQ-**1**, ReSAACQ-**1** and unlabeled peptide. All values are normalized to control cells and reported as mean±S.D. (B) Results of single-cell gel electrophoresis assays on NSCs at 24 h postincubation with 118.4 MBq of ^{99m}TcSAACQ-**1** versus cells incubated with only PBS. Values are reported as mean±S.E.

To produce a radiolabeled permeation peptide that retains its biological activity, we employed a new ligand for ^{99m}Tc that can be incorporated into the backbone of peptides as if it were a natural amino acid. The single amino acid chelate (SAAC) forms a well-defined product upon labeling that is stable, thereby preventing any chance of premature loss of the isotope in vivo [23–25]. Because it is an amino acid analogue, peptides containing the SAAC can be prepared in large quantities using a conventional automated peptide synthesizer. Another advantage of the SAAC system is that the nonradioactive Re analogues, which are needed as reference standards for the ^{99m}Tc-labeled peptides, can also be prepared on the automated synthesizer following the same procedures used to prepare the SAAC-peptide derivative. For the purposes of the present study, the SAACQ (SAAC-quinoline) ligand [24] (Fig. 1A) was used because its Re complex (Fig. 1B), which is structurally identical to the ^{99m}Tc analogue, is luminescent. This feature, which is unique to this particular ligand system, provided the opportunity to evaluate the cellular uptake and distribution of the target peptide, ReSAACQ-**1**, in neurospheres at high resolution using epifluorescence microscopy prior to preparing the radioactive analogue.

The peptides SAACQ-**1** (Fig. 1C) and ReSAACQ-**1** (Fig. 1D, M=Re) were prepared following conventional Fmoc automated peptide synthesis protocols (Fig. 2). The peptides were released from the resin using a standard cleavage cocktail, and the products were purified by preparative HPLC [26,27]. The purity was confirmed by HPLC, and the nature of the products was verified using mass spectrometry. The presence of the $[Re(CO)_3]^+$ core in ReSAACQ-**1** was also verified by IR spectroscopy, where the distinct CO stretches were observed at 1933 and 2035 cm^{-1}.

Using ReSAACQ-**1**, we determined the uptake and distribution of the probe in vitro using fluorescence microscopy. Suspensions of dissociated neurospheres were incubated with

various concentrations of the probe for different lengths of time, and the microscopy images were acquired (Fig. 3A–C). The probe localized primarily in the cell nucleus with a significant degree of association on the nuclear envelope. A smaller amount was found to be dispersed in the cytoplasm, which is similar to the results reported for an FITC-labeled HIV-Tat analogue [18]. The results clearly indicate that the presence of the ReSAACQ complex in the backbone of the peptide did not have a detrimental influence on the cell-penetrating ability of the targeting sequence.

Having demonstrated that ReSAACQ-**1** was effective at labeling NSCs, we performed quantitative uptake experiments using the ^{99m}Tc analogue. To prepare ^{99m}TcSAACQ-**1** (Fig. 2), we added SAACQ-**1** to a solution of $[^{99m}Tc(CO)_3(OH_2)_3]^+$, which can be synthesized in a single step from the generator product $[^{99m}TcO_4]^-$ using an instant kit [28]. The product can be isolated in both low and high effective specific activities where the latter was achieved using semipreparative HPLC, giving the desired peptide in excellent radiochemical purity (>98%) in 43±7% yield (n=12). Following purification, the stability of the complex was tested using a ligand challenge experiment where there was no evidence of transchelation when the labeled product was incubated in the presence of a large excess of either cysteine or histidine for 24 h at 37°C.

Varying amounts of ^{99m}TcSAACQ-**1** were subsequently incubated with dissociated neurospheres as a function of time. Following copious washing, uptake was determined by measuring the amount of activity in the final cell pellet and conservatively assuming the number of cells present to be the same as at the start of incubation. Uptake levels ranged from 2 to 367 Bq of ^{99m}TcSAACQ-**1** peptide per cell (1.0×10^{-19} to 1.9×10^{-17} mol/cell) with average values ranging between 10 and 20 Bq/cell, which is significantly higher than for most cell-tagging methods. Cell loading levels were however somewhat variable, which we propose is the result of difficulties in achieving identical levels of neurosphere dissociation across all experiments.

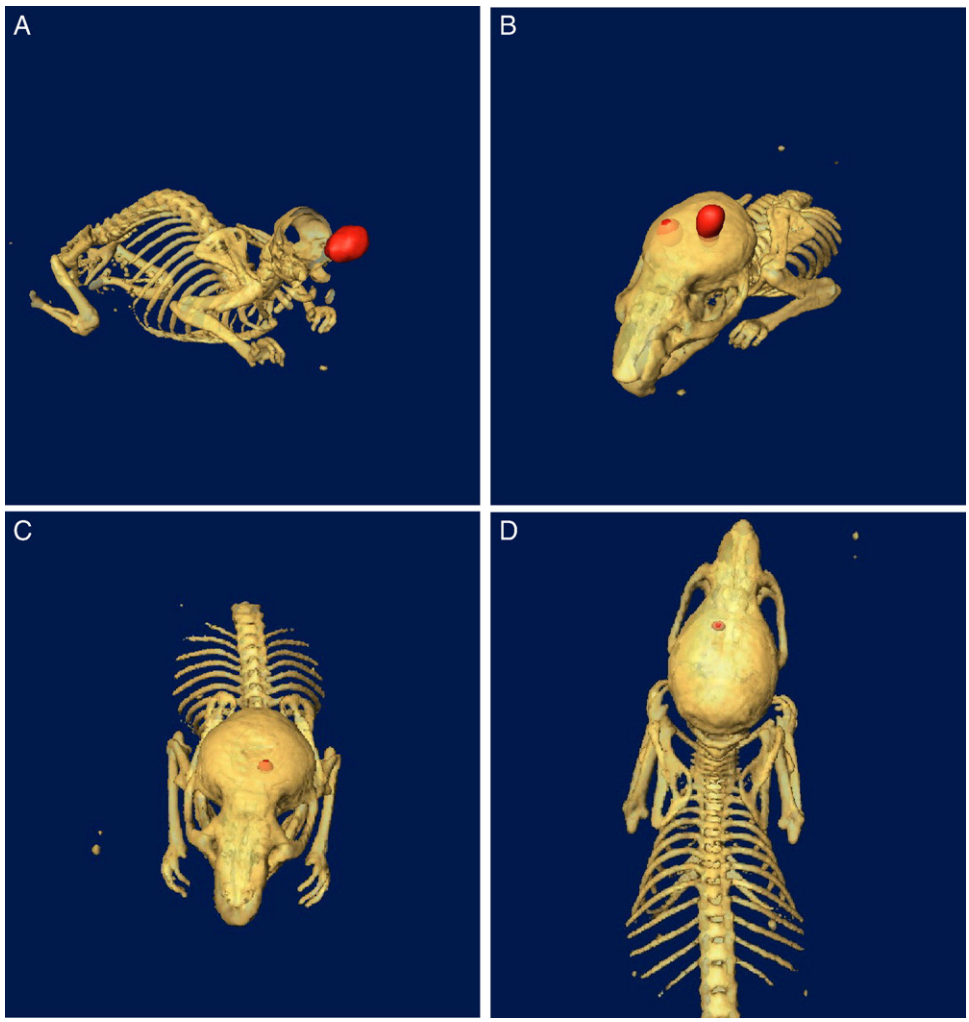

Fig. 5. SPECT/CT images of bilateral transplants: (A) parallel-hole collimator image with the CT image of the skull removed (11 Bq/cell); (B) 15 h postmortem SPECT/CT image using a pinhole collimator of the same animal described in Panel A. (C and D) Two-hour pinhole SPECT/CT image of a bilateral transplant of 841±43 cells containing 10 Bq/cell (cells were detected in only one transplantation site).

Washout studies were also performed in order to assess efflux of ^{99m}Tc from the cells following labeling and initial washing. A loss of activity was detected for the first 20 min; however, after that point, 57±7% (n=12) of the activity remained within the cells, which is consistent with data from other HIV-Tat-based probes [20]. In spite of the loss, the net uptake was still greater than the values reported for other cell radiolabeling procedures.

As determined by colorimetric cell-exclusion assays, viability for cells labeled with high effective specific activity ^{99m}TcSAACQ-**1** was 97±4% at 2 h postlabeling and 85±25% at 24 h postlabeling (Fig. 4A) for incubation activities ranging from 245 to 8900 Bq/cell. However, when the incubation amounts per cell were further increased, there was a substantial drop in cell viability. This is likely due to increased radiolytic damage and not to the increased amount of ligand since viability at these levels of activity in the presence of additional amounts of free peptide was not decreased further.

While colorimetric cell-exclusion assays allow for the determination of cell viability in terms of membrane integrity, they do not provide any information regarding DNA damage, which might arise during incubation or as a result of intracellular deposition of the radionuclide. In order to determine whether any DNA damage occurred in the presence of ^{99m}TcSAACQ-**1**, we analyzed labeled cells by single-cell gel electrophoresis [29,30]. Cells were incubated with similar amounts of activity used for the colorimetric viability studies and the extent of DNA damage compared to PBS-treated control cells (Fig. 4B). The experiments showed that there was no significant difference between the extent of DNA damage in the treated cells versus control cells, indicating that the presence of ^{99m}TcSAACQ-**1** at high effective specific activity does not induce any additional damage to DNA within 24 h of incubation. Unfortunately, it was not possible to compare these results to other studies involving different cell-labeling strategies as this level of DNA analysis is not typically reported.

For all transplantation experiments, cells were labeled using the tracer prepared at high effective specific activity. Cells were prepared in 3 μl of lactated Ringer's solution for stereotaxic injection into the striatum of mice. For the first imaging study, a bilateral transplant of cells (11 Bq/cell after washout) into the striatum of a healthy mouse was performed. Static-planar and low-resolution SPECT/CT images were collected using a parallel-hole collimator at 20 min posttransplantation. These studies showed that 3-D images of cells labeled with 11 Bq/cell could be readily visualized (Fig. 5A). Using a calibration curve and selecting the appropriate region of interest on the planar image, we determined that 5656±446 cells containing a total of approximately 7.4×10^4 Bq of activity were successfully transplanted. Following euthanasia, an extended (15 h) high-resolution image using a pinhole collimator was collected (Fig. 5B). These images show activity residing on the surface of the skull, which is an indication of labeled cells residing outside of the brain. This is likely due to extrusion of the cells upon removal of the transplant needle.

A second study was initiated to determine if the high-resolution images could be obtained in a shorter period of time using a smaller number of cells and without having to euthanize the subject. A mouse was anesthetized and subjected to a bilateral transplant with cells containing 10 Bq/cell. Pinhole images were acquired (Fig. 5C and D) for 2 h, after which the mouse was allowed to recover from the anesthetic. For this particular study, it was apparent that only one of two transplant sites contained an adequate number of cells/activity for detection. This was not totally unexpected given the tendency of such a small number of cells to adhere to the implant syringe. From a static-planar image, it was determined that 841±43 cells were successfully implanted into the single injection site. The mouse recovered fully

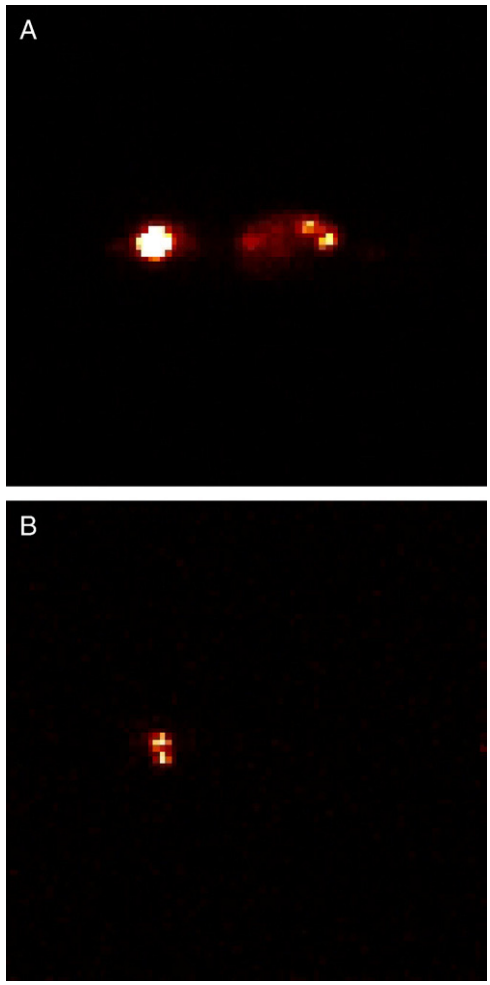

Fig. 6. Static-planar images following (A) bilateral intracranial injection of 1.85 MBq of a solution of ^{99m}TcSAACQ-**1** and (B) bilateral transplant of approximately 5656±446 cells containing 11 Bq/cell of ^{99m}TcSAACQ-**1**. The peptide-only injection shows that while the majority of the activity remains in the brain, a significant amount does migrate into the abdominal region while the labeled cells reside primarily in the striatum of the mouse.

from the procedure, suffering no adverse effects, indicating that this technique can be used to noninvasively monitor the intracerebral transplantation of even a very small number of NSCs.

For comparison, the peptide ^{99m}TcSAACQ-**1** alone was injected into the brain of a mouse using a procedure similar to that used for the labeled cells. The resulting images show, as expected, more widespread distribution of the free tracer compared to that for the labeled cells. Activity was initially concentrated in the brain; however, at 10 min postinjection, there was accumulation of activity in the abdominal region of the mouse. This increased with time with a subsequent scan at 15 h postinjection showing a significant degree of localization in the stomach (Fig. 6).

With the cell-labeling and SPECT/CT techniques in hand, additional imaging studies following a number of different transplant procedures were performed. The extent and position of cell implants were readily monitored and found to be highly variable, including cases where bilateral transplants ended up being placed closer together than was expected. These results are in agreement with literature reports on the poor efficiency and reproducibility of cell transplants, while at the same time they highlight the advantages of using small-animal imaging to assess and optimize procedures.

4. Conclusions

The methodology reported here is a convenient strategy for monitoring neurosphere transplantations in small-animal models. The technique can be used to verify the position of the cells and to give an estimate of the number transplanted. The fact that the labeling system is based on ^{99m}Tc makes the reported approach readily accessible and inexpensive, and imaging studies can be performed over 24 h while still imparting a low dose burden on the subject. For preclinical studies, this latter point is an important consideration particularly when sensitive animal models and/or multiple transplant procedures are to be used. Although trafficking studies are important, accurate methods for assessing transplants on a case-by-case basis could, in the long term, have a more significant impact on the ultimate success of NSC therapies.

Acknowledgments

The imaging studies were made possible by the acquisition of a GammaMedica X-SPECT scanner, which was purchased with funding from Hamilton Health Sciences and McMaster University. The authors gratefully acknowledge support from the Ontario Research and Development Challenge Fund, The Canadian Foundation for Innovation and the Ontario Innovation Trust. We also wish to acknowledge the Natural Sciences and Engineering Research Council for awarding a scholarship to J.A.G.

References

[1] Doetsch F, Caillé I, Lim DA, García-Verdugo JM, Alvarez-Buylla A. Subventricular zone astrocytes are neural stem cells in the adult mammalian brain. Cell 1999;97:703–16.
[2] Goldman S. Stem and progenitor cell-based therapy of the human central nervous system. Nat Biotech 2005;23:862–71.
[3] Lundberg C, Winkler C, Whittemore SR, Björklund A. Conditionally immortalized cells grafted to the striatum exhibit site-specific neuronal connections with the host globus pallidus. Neurobiol Dis 1996;3: 33–50.
[4] de Vries IJM, Lesterhuis WJ, Barentsz JO, Verdijk P, van Krieken JH, Boerman OC, et al. Magnetic resonance tracking of dendritic cells in melanoma patients for monitoring of cellular therapy. Nat Biotech 2005;23:1407–13.
[5] Frangioni JV, Hajjar RJ. In vivo tracking of stem cells for clinical trials in cardiovascular disease. Circulation 2004;110:3378–84.
[6] Ma B, Hankenson KD, Dennis JE, Caplan AI, Goldstein SA, Kilbourn MR. A simple method for stem cell labeling with fluorine 18. Nucl Med Biol 2005;32:701–5.
[7] Brenner W, Aicher A, Eckey T, Massoudi S, Zuhayra M, Koehl U, et al. ^{111}In-labeled CD34+ hematopoietic progenitor cells in a rat myocardial infarction model. J Nucl Med 2004;45:512–8.
[8] Chin BB, Nakamoto Y, Bulte JWM, Pittenger MF, Wahl R, Kraitchman DL. ^{111}In oxine labelled mesenchymal stem cell SPECT after intravenous administration in myocardial infarction. Nucl Med Commun 2003;24:1149–54.
[9] Aicher A, Brenner W, Zuhayra M, Badorff C, Massoudi S, Assmus B, et al. Assessment of the tissue distribution of transplanted human endothelial progenitor cells by radioactive labeling. Circulation 2003; 107:2134–9.
[10] Bai J, Ding W, Yu M, Du J, Liu Z, Jia B, et al. Radionuclide imaging of mesenchymal stem cells transplanted into spinal cord. Neuroreport 2004;15:1117–20.
[11] Ford JW, Welling III TH, Stanley JC, Messina LM. PKH26 and 125I-PKH95: characterization and efficacy as labels for in vitro and in vivo endothelial cell localization and tracking. J Surg Res 1996;62:23–8.
[12] Gao J, Dennis JE, Muzic RF, Lundberg M, Caplan AI. The dynamic in vivo distribution of bone marrow-derived mesenchymal stem cells after infusion. Cells Tissues Organs 2001;169:12–20.
[13] Zhou R, Thomas DH, Qiao H, Bal HS, Choi S-R, Alavi A, et al. In vivo detection of stem cells grafted in infarcted rat myocardium. J Nucl Med 2005;46:816–21.
[14] Jin Y, Kong H, Stodilka RZ, Wells RG, Zabel P, Merrifield PA, et al. Determining the minimum number of detectable cardiac-transplanted ^{111}In-tropolone-labelled bone-marrow-derived mesenchymal stem cells by SPECT. Phys Med Biol 2005;50:4445–55.
[15] Kizilian N, Wilkins RC, Reinhardt P, Ferrarotto C, McLean JR, McNamee JP. Silver-stained comet assay for detection of apoptosis. Biotechniques 1999;27:926–8.
[16] Zhao M, Kircher MF, Josephson L, Weissleder R. Differential conjugation of tat peptide to superparamagnetic nanoparticles and its effect on cellular uptake. Bioconjug Chem 2002;13:840–4.
[17] Wunderbaldinger P, Josephson L, Weissleder R. Tat peptide directs enhanced clearance and hepatic permeability of magnetic nanoparticles. Bioconjug Chem 2002;13:264–8.
[18] Bhorade R, Weissleder R, Nakakoshi T, Moore A, Tung CH. Macrocyclic chelators with paramagnetic cations are internalized into mammalian cells via HIV-Tat derived membrane translocation peptide. Bioconjug Chem 2000;11:301–5.
[19] Lewin M, Carlesso N, Tung C-H, Tang X-W, Cory D, Scadden DT, et al. Tat peptide-derivatized magnetic nanoparticles allow in vivo tracking and recovery of progenitor cells. Nat Biotech 2000;18: 410–4.
[20] Gao X, Yang L, Petros JA, Marshall FF, Simons JW, Nie S. In vivo molecular and cellular imaging with quantum dots. Curr Opin Biotech 2005;16:63–72.

[21] Polyakov V, Sharma V, Dahlheimer JL, Pica CM, Luker GD, Piwnica-Worms D. Novel Tat-peptide chelates for direct transduction of technetium-99m and rhenium into human cells for imaging and radiotherapy. Bioconjug Chem 2000;11:762–71.

[22] Säälik P, Elmquist A, Hansen M, Padari K, Saar K, Viht K, et al. Protein cargo delivery properties of cell-penetrating peptides. A comparative study. Bioconjugate Chem 2004;15:1246–53.

[23] Banerjee SR, Levadala M, Lazarova N, Wei L, Valliant JF, Stephenson KA, et al. Bifunctional single amino acid chelates for labeling of biomolecules with the {$Tc(CO)_3$}+ and {$Re(CO)_3$}+ cores. Crystal and molecular structures of [$ReBr(CO)_3(H_2NCH_2C_5H_4N)$)], [$Re(CO)_3\{(C_5H_4NCH_2)_2NH\}$]Br, [$Re(CO)_3\{C_5H_4NCH_2)_2NCH_2CO_2H\}$]Br, [$Re(CO)_3\{X(Y)NCH_2CO_2CH_2CH_3\}$]Br (X=Y= 2-pyridylmethyl; X=2-pyridylmethyl, Y=2-(1-methylimidazolyl) methyl; X=Y=2-(1-methylimidazolyl)methyl), [$ReBr(CO)_3\{(C_5H_4NCH_2)NH(CH_2C_4H_3S)\}$], and $Re(CO)_3\{C_5H_4NCH_2)N(CH_2C_4H_3S)(CH_2CO_2)\}$]. Inorg Chem 2002;41:6417–25.

[24] Banerjee SR, Wei L, Levadala MK, Lazarova N, Golub VO, O'Connor CJ, et al. {ReIIICl3} core complexes with bifunctional single amino acid chelates. Inorg Chem 2002;41:5795–802.

[25] Stephenson KA, Banerjee SR, Besanger T, Sogbein OO, Levadala MK, McFarlane N, et al. Bridging the gap between in vitro and in vivo imaging: isostructural Re and ^{99m}Tc complexes for correlating fluorescence and radioimaging studies. J Am Chem Soc 2004;126:8598–9.

[26] Kiso Y, Satomi M, Ukawa K, Akita T. Efficient deprotection of NG-tosylarginine with thioanisole-trifluoromethanesulphonic acid system. Chem Commun 1980:1063–4.

[27] Atherton E, Sheppard RC, Ward P. Peptide synthesis. Part 7. Solid-phase synthesis of conotoxin G1. J Chem Soc Perkin Trans I 1985: 2065–73.

[28] Alberto R, Schibli R, Egli A, Schubiger AP, Abram U, Kadtem TA. A novel organometallic aqua complex of technetium for the labeling of biomolecules: synthesis of $[^{99m}Tc(OH_2)_3(CO)_3]^+$ from $[^{99m}TcO_4]^-$ in aqueous solution and its reaction with a bifunctional ligand. J Am Chem Soc 1998;120:7987–8.

[29] McNamee JP, McLean JRN, Ferrarotto CL, Bellier PV. Comet assay: rapid processing of multiple samples. Mutat Res 2000;466:63–9.

[30] Ryan LA, Wilkins RC, McFarlane NM, Sung MM, McNamee JP, Boreham DR. Relative biological effectiveness of 280 keV neutrons for apoptosis in human lymphocytes. Health Phys 2006;91:68–75.